Hole-doping of Fullerenes and Nanotubes by way of Intercalation Chemistry

D. Claves

Université B. Pascal, Laboratoire des Matériaux Inorganiques
24 Av. des Landais, 63177 Aubière Cedex, France

E-mail : daniel.claves@univ-bpclermont.fr

Tel.: +33 473 407 647 Fax: +33 473 407 108

Received: 31 January 2006. Accepted: 30 May 2006

Contents:

Abstract: Succeeding to the electron-doping processes of carbon nanostructures, chemical methods devoted to the hole-doping of the latter have significantly developed over the past ten years. Intercalation chemistry remains a top-rated technique in this purpose, among the variety of available chemical doping schemes. A review of the p-type doping of fullerenes and nanotubes by this method is exposed, which also includes a wide range of potential applications and prospects regarding the materials thus obtained.

Keywords : Fullerenes, Carbon Nanotubes, Nanomaterials, Intercalation, p-type doping, Acceptors

1. INTRODUCTION – GENERAL ASPECTS

The polymorphism of carbonaceous materials is at the source of various properties which make them interesting precursors for many technological applications. Through its different crystalline forms, carbon is the unique element whose electronic properties can smoothly cover the insulating to semi-conducting and metallic states range. Additionally, it turns out that the different unsaturated bonding schemes often present in a carbon network confer to this element a high chemical reactivity. Hence, additional band gap modulation can be exerted by chemical modification of a carbon allotrope. From the terminology standpoint, "doping" has been indifferently used to evoke either substitution or intercalation reactions and sometimes, though rather improperly, even addition reactions, in this case.

The true control of the electronic properties of a carbonaceous precursor by external functionalization supposes a regular distribution of motifs over its surface, making band gap engineering unlikely to be realized by this means. Alternatively, the effect searched for may be obtained with minimal alteration of the initial structure through substitutional solid solutions involving boron or nitrogen, but the procedure may suffer from the difficulty encountered with the control of the final composition and from the random order that results. The latter problem has been partially solved only in the case of fullerenes, with the help of advanced synthesis patterns elaborated by organic chemists. In contrast with the previous methods, intercalation chemistry happens to be more flexible and often affords easy control of the doping level or structural periodicity, via simple synthesis routes, and remains up to date the most customary strategy employed for tuning the Fermi level in carbon materials.

Somehow, if the amphoteric character of graphene sheets in regard to electron acceptance or donation has been illustrated throughout a plethora of examples, the electronic effects induced by curvature and confinement of the π electrons will obviously alter such a property in the curved carbon lattices i.e. fullerenes and nanotubes. Thus, most of the time driven by a several decades long earlier background dedicated to the intercalation chemistry of graphite and graphite fibres, intensive work on the doping by the same way, of these new carbon allotropes, has been performed since early 1990's. Earlier reviews [1-3] on the subject essentially described the intercalation of carbon nanotubes or fullerenes with electron donors, including sometimes incipient results with some acceptors. Henceforth, solid foundations devoted to their p-type doping have been laid and motivate the present focus on the highlights that have emerged in this field over the past ten years. The present synthetic approach compiles, in a first part and in an as exhaustive as possible way, the main experimental results reported to date concerning the recently appeared hole-doping of carbon nanotubes via intercalation chemistry. During the lull that followed the resounding success of the n-type doping of fullerenes, novel doping schemes were developed, which have seemingly not been paid the attention they may deserve and which will be dealt with in the second section of this article. Beside the conventional narrative description of the essential conclusions of each relevant publication examined, some critical considerations have been introduced from time to time. Given the abundant literature in materials science relating to fullerenes and nanotubes, efforts were made to refer to as general as possible references in the introductory parts, whenever possible.

This review remains restricted to what may be qualified as condensed-phase oxidative intercalation chemistry, which implies core diffusion of a guest-species into the carbon host lattice under consideration, the doping effect arising from the subsequent development of a strong interaction between the dopant and matrix electronic states, leading to net charging of the imbricated sublattices. Therefore, it does not include results related with gas adsorption, solution redox chemistry, surface electrochemical doping involving the formation of a

charged double layer, also termed capacitive charging, or still voltage-induced hole-doping, sometimes termed gate voltage charging.

2. THE P-TYPE DOPING OF CARBON NANOTUBES

2.1. Single-walled carbon nanotubes (SWNTs)

We will first briefly recall the main characteristics of SWNTs in the condensed state and the essential investigation techniques retained for their study and the one of their derivatives, as well as their proper justification. No distinction will be introduced, in the following, between batches issued from the two essential elaboration techniques available yet i.e. laser vaporization or CVD, though the related diameter characteristics are essentially different.

From a structural standpoint, a SWNT represents one of the building blocks of the regular hexagonal close-packing of cylinders constituting a crystalline rope of SWNTs, whose self assembly is ensured through van der Waals interactions. Thus, beside variations in diameter and/or helicity, the presence of not necessarily correlated orientations from tube to tube implies an absence of true long range order in the stacking of these individual entities and the overall matrix can only be described on the basis of an average continuum.

Regarding intercalation phenomena into such a medium, X-Ray diffraction (XRD) basically remains the main tool of investigation but can only give access to limited information, owing to the absence of fine structures arising from the statistical disorder of the carbon host-lattice under consideration, to its low scattering power, and above all to short coherence lengths in the material which result in ill-defined Bragg peaks. For such reasons, direct observation via transmission electron microscopy (TEM) is often complementarily employed, when possible, but specific problems related to a sometimes limited stability of an intercalation compound under high vacuum, under the electron beam or a not attainable atomic scale resolution make it not necessarily more adequate than XRD. Therefore, to which extent structural order within an intercalated SWNTs bundle is achieved still remains an open question, most of the time. Figure 1a-c gives a panel of the different scenarios that could be envisaged, given the various structural sites available to an intercalant species. Note that mixed situations are not precluded. Whether the conventional staging concept, inherent to the intercalation chemistry of lamellar compounds, can be applied to such a pseudo 1D-matrix remains another aspect to integrate in a clear global vision of the intercalation chemistry of SWNTs ropes. Some relevant energy aspects have been shortly addressed in a previous paper by Fischer [4].

Some authors propose to consider a carbon nanotube rather as an individual aromatic macromolecule, endowed with its own intrinsic properties, and such an individuality has to be accounted for in the description of the related bulk state, especially when dealing with the electronic properties of the latter. It may be necessary here to once again insist on the fact that the properties stemming from the doping process of SWNTs ropes should then not be interpreted as a uniform collective behaviour but rather as an averaged sum over all individual behaviours. Somehow, a unifying description may from time to time be attempted, given the similar electronic states distribution encountered from tube to tube, which obeys a universal scheme. Indeed, due to the one-dimensional character of each separate tubular edifice, the DOS consists in a mirror spikes distribution [5] (fig. 2a), known as van Hove singularities.

Consequently, the most prominent features observed in optical absorption spectroscopy (OAS) arise from electronic transitions between these singularities. In practice,

the characteristic absorption spectrum of SWNTs can usually be decomposed into three main contributions [6,7] falling in the visible and near-infrared ranges (fig. 2b), corresponding to the first two optically allowed interband transitions issuing from an apparently single averaged semi-conducting tube, and to the energy separation between singularities in the valence and conduction bands of an apparently single averaged metallic tube, respectively. Variations in the DOS from tube to tube simply cause a broadening effect. On such grounds, any modification affecting the transitions between the nearly molecular-like levels fairly reflects the changes occurring in the average electronic structure, within a rigid band framework, however. OAS has therefore often been used as an efficient qualitative probe of such changes in the electronic structure, following a doping-induced charge transfer.

Known as an often essential characterization technique of carbonaceous materials, Raman spectroscopy has turned out to be more than ever crucial for the study of carbon nanotubes. One may refer to comprehensive literature [8] written by experts in the field, for an overview on the subject. Basically, Raman scattering for carbon nanotubes is essentially a resonant process, in other words the scattered intensity is enhanced when the laser wave length matches the energy gap associated with a van Hove singularity pair in the above-described 1D electronic DOS. The first consequence is a selective response from only those few tubes whose electronic structure can satisfy the resonance condition. The latter phenomenon may represent a drawback, since using different laser excitation energies becomes necessary for obtaining collective data, but it is also advantageously used as a specific observation means of isolated individuals.

Two main Raman active modes, well separated in frequency, have to be distinguished. The former components are related to the symmetric atomic displacement along the radial direction (the so-called radial breathing mode RBM, ~ 200 cm^{-1}), and to anti-symmetric vibrations along the tube axis and circumference (the tangential modes TM, ~ 1600 cm^{-1}), respectively. As the latest is characteristic of sp^2 carbons, it is sometimes also referred to as the G mode, by analogy with graphite. The frequency of the first mode happens to be highly diameter sensitive, varying as a function of the inverse of the value of the latter. Concordant scales have been established [8]. This mode is naturally used as a probe to characterize any diameter-dependent properties, i.e. to discriminate between metallic and semi-conducting tubes responses within a mixed sample, through the diameter / chiral indices / metallicity interconnection.

Regarding doping, the TM turn out to be particularly useful to at least semi-quantitatively analyse charge transfer phenomena, as experimented earlier with graphite salts, for instance. Any shift of the corresponding stretching frequency indeed reflects a change appearing in the strength of the carbon-carbon bond, which is directly proportional to the local electron density. Thus, positive ionization, which reduces electron screening, reinforces the internal bonding scheme of a carbon host lattice and is associated with systematic upshifting effects. Advantage can even be gained relative to a formal measure of charge transfer amounts. One may here emphasize the non-universality of the method regarding carbon nanotubes, since the former trend seems prone to irregular variations when these are associated with electron donors. It may be useful to precise that charge transfer in carbon nanotubes also usually results in a strong attenuation of the absolute intensities of the Raman spectral lines, due to a gradual quench of the optical transition responsible for resonance, in the course of the filling, with either electrons or holes, of the levels involved in it.

2.1.1. Halogens

Br_2 : Bromine is recognized as an archetype of acceptor molecule, when accommodated inside a host carbon lattice, a fact probably intimately related to the reason why this halogen has been at the source of the pioneering attempts [9-11] devoted to the p-type doping of carbon nanotubes. Thus, SWNTs bundles exposed to bromine vapour were found to exhibit a drastic enhancement of their electrical conductivity [9], an effect conventionally interpreted in terms of electron donation to the bromine species. The samples were also able to undergo doping/de-doping cycles upon successive heating in air and bromine re-exposure. Complete halogen removal seemed quite difficult to obtain, however, and suggestive of the existence of stable intermediate phases of fixed composition, recalling the staging phenomenon encountered with graphite intercalation compounds (GICs). The partial ionic character of carbon was simultaneously confirmed through a substantial blue shifting of the highest frequencies Raman features [10,11], illustrating strengthening of the C-C bond that followed a doping-induced diminution of the electron density in the vicinity of carbon atoms.

In order to better assess the changes appearing in the electronic structure upon Br-doping, one may retain the following sketchy view issuing from a rigid band representation of the latter. According to the interpretation of OAS data [7, 12-14] (fig. 3), a progressive electron depletion of the highest occupied states with increasing acceptor concentration is evidenced by the extinction of the absorption bands involving these levels, while at the same time, the shift in the Fermi energy gives birth to new allowed electronic transitions between some low lying states and the doping-induced depopulated zone within the primary DOS, adding novel features to the spectrum. Some independent theoretical calculations [15] showed that depending on the average intermolecular distance between supposedly sorbed Br_2 species at outer surfaces within a bundle, which is a direct function of bromine concentration in the sample, the antibonding states-derived band of bromine may indeed overlap with the carbon π band, leading to a metallic state accompanied by more or less pronounced electron transfer from carbon to bromine. However, as outlined by the authors, the model was based on not necessarily optimized disposition and chemical nature of the intercalant, since molecular bromine was considered.

I_2 : The results of a gas-phase doping with molecular iodine remain controversial. Some noted small to insignificant changes in the electronic properties [10-12], whereas others depicted effects similar to doping by bromine [7,13,14]. The divergence may arise from more or less efficient chemical doping procedures.

Chronologically, the most relevant contribution dealing with the intercalation of iodine within SWNTs bundles should be ascribed to Eklund and coll. [16], who largely drew their inspiration from the earlier studies on the doping of one-dimensional organic polymers. In a thorough preliminary investigation, these authors thus showed that reacting SWNTs with molten-iodine yields, after subsequent annealing, a phase with composition close to IC_{12} at saturation. From a structural standpoint, XRD revealed an expansion of the bundles upon intercalation, suggesting occupation of the intertubular van der Waals gaps by the intercalant. Partial to complete disorganization of the initial regular stacking present within the carbon host lattice arose when the doping level was increased, and appeared only partially reversible when a heating-induced de-intercalation procedure was attempted.

Some characteristic Raman and XPS signatures revealed the chemical nature of the intercalated species, which evolves from anionic I_3^- to I_5^- oligomeric chains, when approaching saturation. The presence of negatively charged complexes then necessarily implies an effective charge transfer toward the guest species, which again manifested through an upshift, proportional to the doping level, of the tubules' tangential stretching modes in the Raman spectrum, consistently with a lower electron density at carbon sites. The transport properties were found to be strongly affected by the charge transfer effect in that the iodine-

doped materials exhibited a notable increase in electrical conductivity over the 20-300 K temperature range. An unexpected positive $(dR/dP)_T$ slope was also later reported [17] during the measurement of the average resistance under hydrostatic pressure, which remained unexplained.

As the structural information delivered by XRD remains limited, the same group attempted a direct observation of the spatial distribution of iodine by Z-contrast scanning transmission electron microscopy and established [18] unambiguously the filling of the central cavity by twisted pairs of polyiodide chains, beside occupation of the intertubular channels. The former helical conformation may originate from the better commensurability that results in the matching of both iodine and carbon sublattices. In a further study [19], after careful attribution of part of the low frequency Raman spectrum of iodine-doped SWNTs samples once again to the response of intercalated polymeric iodine, it was suggested that both the shifting and non-shifting effects observed under pressure on the latter signals may arise from different location of the iodine chains within the bundles, i.e. the pressure-independent features should be assigned to a part of iodine residing in the hollow core of some tubes, thus confirming the earlier more direct observation. A more recent independent work [20], combining X-ray and neutron diffraction techniques, and therefore allowing the separation of the contributions to diffraction of the respective light and heavy element sublattices, confirmed the major intra-tube and minor extra-tube localization of iodine.

2.1.2. Brönsted acids and their conjugated bases

Carbon can be maintained in an oxidized state in the presence of a non-reducing counter anion, such as an oxoanion in which the oxidation state of the central atom is maximal. This is well exemplified by the formation of graphite salts, which were among the earliest GICs reported. Whereas their preparation requires an external supply of free energy or the presence of a strong oxidant, the synthesis of analogous phases from carbon nanotubes seems to readily proceed.

HNO_3: Thus, simply refluxing SWNTs samples in nitric acid over short time periods gave further structural evidence that bundles can be reversibly intercalated with guest-species [21, 22], while maintaining some kind of long range order. XRD indeed formally established an increase in the intertube distance, in this case, implying insertion into the carbon network. Such an expansion of the associated close-packed triangular lattice creates enough available free space to allow accommodation of HNO_3 molecules in the interstitial channels. The latter can be reversibly extracted by subsequent annealing, though the process leaves some residual disorder and can be responsible for noticeable bundles exfoliation. Strictly similar results were also later reported [23] from an electrochemical intercalation procedure. It was independently found [24], on the basis of typical IR signatures, that beyond 300 °C, partial conversion of some intercalated nitrate anions into covalently bound nitro-groups can occur.

Not surprisingly, the classical quenching of some optical absorption features [24, 25] illustrates the creation of holes in the carbon π states, following nitric acid treatment. From a mechanistic point of view, it is highly unlikely that the phenomenon observed arises from N(+V) acting as a true oxidant. Though this critical point is never tackled in the literature, the spontaneous reaction should probably not be seen as resulting from a redox process but rather from the protonation of the π electrons system. Thus, once again, a stiffening of the Raman modes was found to accompany such a pseudo-electron transfer to the acid molecule [22, 26, 27]. Various techniques have afterwards been employed [28, 29] to quantitatively establish a ≈ 0.3 eV downshift of the carbon network Fermi level, induced by doping with HNO_3. It was also suggested [30] that the successively growing and diminishing Dysonian character of the EPR

signals, respectively recorded after i) acid treatment and ii) heat treatment ensuring removal of the intercalated molecules, reflected an evolution in the free charge carriers concentration. More direct evidence of an increased density of conduction electrons in such samples were provided by a strong absorption in the far-IR [25] or by resistivity measurements [29].

In spite of the appealing aspects described above, attention should be paid to the fact that mineral oxyacids have also long been known as efficient reagents for the functionalization of carbon surfaces, which still holds true for carbon nanotubes. The use of nitric acid therefore generates side reactions. Prolonged treatments have also shown to even induce destruction of some tubes [21, 22], which can turn into various multi-shell phases as a consequence of oxidative etching followed by internal reorganization.

H_2SO_4: The first study mentioning intercalation of a Brönsted acid into a SWNTs rope lattice aroused emulation within part of the scientific community that had previously been involved in the GICs chemistry, and was soon after followed by the doping of SWNTs bundles with sulfuric acid [31, 32]. Thus, these were found to spontaneously react with concentrated H_2SO_4, resulting in the formation of the bisulfate anion associated to the positively charged carbon lattice as counter-ion. A higher doping level could be achieved via moderate electrochemical oxidation, and was explained as an overcharging effect which results from the creation of holes in the carbon π band, simultaneously accompanied by the dissociation of some neutral co-intercalated acid molecules, giving additional HSO_4^- species necessary for global charge compensation. The proper justification came from the negligible mass variation occurring at the electrode, a fact consistent with the conversion of H_2SO_4 molecules to the bisulfate anions which releases dihydrogen only. Whereas the first overcharging regime turns out to be fully reversible, as again later on confirmed by cyclic voltammetry [33, 34], SWNTs become irreversibly oxidized by excessive anodic polarization due to the formation of C-O bonds and even rupture of the carbon frame [31-34]. The analogy with the homologous graphite salt seems then complete, except for the initial non bias-induced reaction observed, whose origin is elucidated below.

Charge transfer was characterized by the now usual significant upshift of the Raman active tangential vibration mode [31, 32]. Since the galvanostatic conditions used allowed Coulometric titration, it became possible to establish the proportionality ratio, provided a linear relation can be verified, between the amplitude of the shift and the amount of charge transfer, which had never been done before. The authors employed several methods aiming at subtracting the contribution from the previously mentioned non-electrochemically assisted reaction that occurs simultaneously, either by making the electrochemical contribution to the overall charge-transfer rate dominant upon drastic increase of the cell current, or by studying the time dependence of the shifting effect at constant intensity, or still by suppressing the undesired perturbation through dilution of the electrolyte. Concordant values, set between 315 and 348 cm^{-1} per hole per carbon atom, were determined. It is however not clear why no attempt was made to study one by one each effect, by letting the spontaneous "oxidation" complete to its end, which seems to take only a few hours and which would probably have led to still slightly better accuracy. Thus, as proposed by the authors, adopting the former value as a universal parameter would provide a quantitative means to measure the charge transfer in SWNT-derived intercalation compounds with acceptors. Dresselhaus and coll. [35] recently suggested that such a quantitative information could also be obtained by using a high frequency second order signal as reference, shifting more sensitively by 423 cm^{-1}/hole/carbon atom. By selectively recording the response of either metallic or semi-conducting tubes, i.e. by varying the energy of the incident light, it was also found that the electrochemically assisted oxidation of metallic tubes in aqueous sulfuric medium proceeds smoothly, whereas that of semi-conducting tubes requires a significantly higher electrochemical potential, which

is consistent with the difference in the Fermi level positions between each type of tube.

Extrapolating the spontaneous reactivity of SWNTs with dilute or concentrated oxyacids solutions to super-acidic conditions led to the recent discovery of their extremely high solubility in such media [36]. This was interpreted as a consequence of the protonation of the π network [36], which is therefore responsible for the previously evoked spontaneous p-doping effect observed, according to $C + \delta\ AH \rightarrow [(CH_\delta)^{\delta+}, \delta\ A^-]$, and which can also induce some kind of self organization by optimization of the electrostatic interactions that develop between charged tubes [37, 38]. Only electrochemical treatments should then be considered as resulting in a true oxidation of the carbon lattice. The electrical properties of H_2SO_4-"impregnated" samples (as opposed to electrochemically prepared samples) have been recently investigated by Fisher and co-workers [29]. First, a drastic drop in resistivity in regard to undoped samples has been shown (fig. 4). Several transport regimes were characterized vs temperature, though the compounds are intrinsically metallic. When compared to HNO_3-derived homologues, a higher downshift of the host lattice Fermi level has also been evidenced [28, 29], suggesting that the sulfuric acid molecule acts as a more efficient dopant and/or that the doping level is more important in this case. A more effective charge transfer in the presence of sulfate anions was also inferred in an independent electrochemical doping study [39]. Assuming that not simple charging of a double layer took place in the conditions used, the upshift of the G-band frequency with polarization was seemingly delayed in a nitrate containing medium. We will once again point out that the charging mechanism in such conditions is fundamentally different, and a direct connection with the preceding experimental fact is not straightforward.

ClO_4^-: The spectro-electrochemical study [40] of SWNTs films, during their successive cathodic and anodic polarization in electrolytes containing perchlorate anions, demonstrated an amazingly symmetrical dumbbell-shaped evolution of both the resistance and Vis-NIR absorption intensities apart both sides of their respective maximum value, associated with the pristine sample. Considering the reasonable assumption that the oxidation process was likely due to the ClO_4^- anion insertion, while that of the counter-ion occurred during reduction, such results provide a direct experimental illustration of the quasi-symmetrical constitution of the SWNTs band structure. They also constitute a nice demonstration of the amphoteric character of these carbon nanostructures in regard to charge induction.

H_2SO_3: A chemical treatment with a dilute solution of H_2SO_3 was also shown to significantly enhance the conductivity of a SWNTs film at room temperature [41], the effect being even more pronounced than that obtained with concentrated H_2SO_4. Whether a protonation phenomenon, similar to the one encountered in the latter case, may at least in part be responsible for the observed behavior was not discussed. From the excellent qualitative experimental correlation between the amplitudes of the changes in conductivity and position of the Raman spectral lines, or still absorbance in the far IR region, it seems possible to scale the "p-doping power" of a given species, which may be envisaged as a practical tool in band gap engineering.

2.1.3. Lewis acids

Numerous metal halides can react with graphite in the presence of an oxidizing atmosphere, forming charge transfer GICs, in which the ability of the intercalant to interact with the carbon sheets is all the more developed that the metal is in a high oxidation state or coordinated by a strongly electronegative ligand. It rapidly became obvious that such kind of

reactions may be anticipated from tubular carbon nanostructures, soon after the discovery of these latest.

$FeCl_3$: $FeCl_3$ has long been known to spontaneously intercalate into the graphite lattice under mild conditions and has played a key role in the history of carbon lamellar compounds. It is therefore not surprising that this reagent was chosen for the basic tentative combination of a Lewis acid with carbon nanotubes. Hence, intercalation of gaseous $FeCl_3$ into crystalline SWNTs bundles seems to reversibly proceed [43], and induces strong internal disorder in the otherwise regular stacking of cylinders, as a result of the expansion required to make compatible the size of the interstitial channels with the one of the intercalate.

Regarding the optical absorption spectrum of the raw tubes, the progressive suppression of electronic transitions with increasing doping level proved the pumping out of electrons from the valence band. The parallel observation, using EELS, of additional resonance conditions from the C_{1s} core level to the novel empty states (see fig. 5) allowed to establish a severe depression by 1.0 eV of the Fermi level. A corresponding charge transfer of about 0.12 e^- per carbon atom was also derived. Since not explicitly specified, it will be assumed that the charge transfer has the same origin as in the homologous GIC and results from the formation of chlorinated anionic complexes. Though not purely specific to the reaction with ferric chloride, a diameter selective doping process of SWNTs ropes was also claimed [44, 45], and was explained either by an easier diffusion of the dopant species between large tubes or by an easier dilation of bundles composed of thin tubes, as the van der Waals interaction energy between neighbouring tubes is proportional to their diameter. Such a conclusion was reached from a diameter selective loss of the Raman active RBM intensities, upon doping of a sample exhibiting a broad tube size distribution. The former interpretation may be the object of further debate, after a more sensitive doping-induced RBM attenuation has been reported for tubes fulfilling a resonance condition [46].

$SOCl_2$: Unexpectedly, the $SOCl_2$ molecule, alternatively a weak Lewis base, seems to behave as a strong p-dopant [41, 42], creating a large number of mobile hole carriers and thus being placed at the top of the "doping-power" scale previously evoked. Raman and core-level photoelectron spectroscopies both indicated a deficiency of electron density at carbon sites [42] after treatment of a SWNTs sample with thionyl chloride, a fact that may deserve to be paid more attention, given that the S(+IV) oxidation state is otherwise not known as oxidizing. This original finding was interpreted as resulting from the formation of charge transfer complexes with sulfur containing species. One may argue that the dissociation of $SOCl_2$ into $SOCl^+ + Cl^-$ ($K_d \sim 10^{-23}$) or a possible protonation of the carbon lattice following hydrolysis of $SOCl_2$ upon air exposure might participate in a satisfactory explanation of the phenomenon observed, however. It is astonishing that a notable effect on the transport properties was also mentioned upon reaction with H_2SO_3, another S(+IV) compound.

2.1.4. Organic dopants

The either reducing or oxidizing character of some organic molecules is well known, and was already turned to account in the elaboration of charge transfer compounds deriving from a host carbon lattice. This was still recently exemplified through the C_{60}-TDAE combination, which had been the object of many studies in the late 1990's. Probably prompted by the former context, in combination with the worldwide notoriety of earlier experimental successes that led to the discoveries of endohedral fullerenes or of the filling of carbon nanotubes by capillarity, a new born doping scheme of SWNTs has recently appeared, which consists in the integration of organic molecules into their hollow core, alternatively

called “encapsulation”. It turns out that amphoteric doping can thus be efficiently achieved, according to the nucleophilic or electrophilic nature of the organic dopant.

TCNQ: A redox reaction in solution between either deposited or solubilized SWNTs and tetracyano-p-quinodimethane (TCNQ) or its tetrafluorinated derivative ($TCNQF_4$) was first mentioned in the literature [47, 48]. The subsequent encapsulation of several types of such organic molecules inside carbon nanotubes seems to have been reported for the first time three years ago [49], after Takenobu et al. submitted SWNTs samples to different kinds of organic compounds vapours. While no peak shift indicative of bundles expansion was apparent, modifications of the relative intensities in the XRD pattern, as compared to those characterizing the pristine material, could be accounted for by a simulated increase of the electron density in the middle zone of the central cavity. Direct confirmation of the endohedral location of the dopant molecules was further obtained by TEM.

The usual modifications in the optical absorption features, Raman spectra and resistivity, characterizing electron exchange were observed when TCNQ or $TCNQF_4$ were used as dopants. The Raman signature of the $TCNQ^-$ anion could also be observed, thus formally establishing the evidence of hole-doping of the SWNTs. Interestingly, the charge transfer effect was monitored as a function of the electron affinity of several electrophilic molecules, revealing a critical threshold under which no carbon oxidation occurs. Similar conclusions were drawn from reducing agents, putting once again in evidence the amphoteric behaviour of nanotubes. First principles calculations further confirmed the pertinence of a charge transfer formalism in these cases [50-52], a pictorial illustration of which is given in fig. 6. More importantly, the encapsulation process was predicted significantly exothermic, rendering expulsion of the endohedral molecule unfavourable, in normal conditions. The related underlying practical interest is straightforward. Moreover, such an inclusion of molecular entities, which may potentially play the role of scattering centres, was predicted not to affect the ballistic nature of the transport properties within the one-dimensional edifice [52]. The chemical shift, in the N_{1s} XPS spectrum [53] of the TCNQ@SWNT compound, further supported the presence of negatively charged N atoms, while the valence band region provided direct imaging of the depletion of the host π-derived band. The N/C ratio established from the area of the corresponding photoemission lines allowed a first reliable quantitative determination of the doping level, close to C_{28}TCNQ, without precluding fixation of some dopant molecules outside the tubes, however.

2.2. Multiwall carbon nanotubes (MWNTs)

One may deplore the paucity of data dealing with the chemical doping of MWNTs, as compared to that of SWNTs. Most of the studies published to date focus on reactions with alkali metals, with a clear view for a potential application in electrochemical energy storage. Besides, only a few transition metal halides or pure halogens seem to have been considered, so far. The following sections also gather works performed with double-walled carbon nanotubes, whose classification as SWNTs or true MWNTs might be ambiguous.

The traditional structural pattern of a MWNT, as outwardly emerging from the set of parallel and periodic dark fringes observed in TEM (Fig. 7), is a self-assembly of nested closed cylinders, the so-called Russian doll model, in which the interlayer spacing is comprised between 0.340 and 0.345 nm, close to the value characterizing turbostratic carbons. Since it is impossible to maintain the perfect ABAB stacking sequence present in graphite, from a curved honeycomb lattice, the generally accepted picture is that helicity varies between contiguous sheets so that an interlayer separation close to that present in disordered graphite can be preserved, and that at best only geometrical correlations between not more

than a few adjacent layers may be expected. This apparent disorder may be amplified by additional internal degrees of freedom of rotational and/or translational origin. Thus, the diffraction pattern of MWNTs samples can keep on being indexed according to the graphite structure, most of the time. Beside reflections of the (00l) type, inherent to periodicity along the stacking direction, and saw toothed-shaped (hk0) peaks, arising from the hexagonal organization within individual curved planes, the presence of (hkl) lines of general type proves the existence of true short range correlations in the stacking scheme. The layers arrangement perpendicularly to the tube axis is then intermediate between those of the graphitic and turbostratic carbons. The interested reader may refer to a paper by Lambin et al. [54], for details concerning the structural characterization techniques of carbon nanotubes.

MWNTs may then easily be compared to a pseudo-1D analogue of graphite, and the question that should rise to any carbon chemist's mind is how far can the reactivity of MWNTs mimic that of graphite ? Regarding intercalation chemistry, some convergence may be anticipated, provided account is taken of the particular topology in this case, which dictates some geometrical requirements to be fulfilled. These are related to the necessary opportunity of a variation in the interlayer separation for an accommodation of guest-species to take place, which is clearly not possible if a configuration of coaxial closed cylinders is considered. Historically, confrontation with the initial experimental evidence of a truly possible occupation, by alkali metal cations, of the interstitial Van der Waals gap present in MWNTs, led to envisage some kind of discontinuity in the supposedly regular stacking of concentric cylindrical graphene sheets. The first intercalation reaction achieved actually happened to represent a major advance in the knowledge of the structure of MWNTs, bringing to light that the latter may exist under various forms. Schemes allowing a lattice expansion perpendicularly to the tube axis, and therefore an accommodation of guest species, are illustrated on figure 1-d,e. If no such disjunctions are present, only interaction with the outermost or innermost surface should be possible, assuming the intercalate can penetrate into the vacant central cavity in the latter case. It may also be likely that some reagents, especially p-type dopants, which are usually notably oxidizing, have a sufficient etching power to create the second category of defects described in fig. 1-d.

At last, the elaboration process of MWNTs has a strong influence on their local microtexture, and as a consequence, on the efficiency of their doping, which is far from being homogeneous along a tube axis. It is then not scarce to observe partly intercalated tubes.

2.2.1. Halogens

F_2: Chemical bonding within a fluorinated inorganic carbon network is highly versatile, according to the synthesis temperature. The corresponding scheme in graphite fluorides, for instance, is well known to evolve from ionic to covalent. Thus, catalytically assisted low temperature processes yield intercalated fluorine species located between the graphene sheets. The analogous fluorination at room temperature of MWNTs was carried out by Hamwi et al. [55], by means of a home made route employing $HF+IF_5$ as catalysts, and known as extremely robust in regard to graphite fluorination. Though a notable weight uptake indicating fluorine fixation to the carbon lattice, XRD and TEM observations showed a non-homogeneous halogenation pattern, leaving some tubes unreacted. Perturbations in the sole outer layers region seemed to indicate a restricted diffusion of the reagents, intercalation likely taking place near the surface only.

Br_2: A study of the bromination of MWNTs [56] again confirmed the chemical affinity of the bromine element with the surface of a nanotube. Thus, bromine fixation resists to successive washing with CCl_4 and high vacuum treatments, a compelling evidence of the

development of a strong interaction, which was ascribed to the formation of a charge transfer complex. In the absence of further precision, the question that may therefore come to mind is whether covalent bond can not form, as in the case of fullerenes. Direct TEM observations showed residual brominated strips, curiously oriented perpendicularly to the tube axis, and the absence of bromine species intercalated between the curved carbon sheets or filling the central cavity.

In the case of MWNTs, information happens to be more difficult to extract from Raman spectroscopy, because of the broadening of the signals which arises from the overlap of several coaxial shells contributions. On such grounds, particularly interesting is the work performed by Eklund and co-workers [57], on the bromine-doping of double-walled carbon nanotubes. In this case, the reduced number of shells generates the discretization of the otherwise global envelope signal. Owing to the particular bi-layer topology and to the diameter dependence of the bands frequencies, each vibration mode consequently splits into two main sets, specific to inner or outer tubes. Thus, the discrimination made allowed to evidence that only the components related to outer tubes were affected by Br-doping, suggesting location of bromine at the outer surface only. Upshift and intensity drop, solely observed for the outer tubes modes, provided experimental evidence that charge transfer occurs from the outermost carbon atoms only. Such a charge distribution was further confirmed by a simulation of the effect exerted on each inner and outer carbon shell by a bromide anions coverage.

I_2: Intercalation into open-ended MWNTs immersed in a molten iodine medium [58] seems to exhibit some kind of similarity with the doping of SWNTs ropes in the same conditions. Thus, the Raman signature of charged iodine complexes was again identified and vanished upon prolonged annealing of the halogenated samples, which demonstrates the reversibility of the iodine incorporation phenomenon within the carbon lattice. The weak I/C elemental ratio determined by desorption tended to prove that iodine can not access the interlayer space of the tubes. In the absence of a TM shifting effect, the authors concluded in the location of iodine preferentially inside the tubes, an argument based on the fact that the predominant contribution to the latter feature should arise from the outermost wall, which is not necessarily true, however.

Sauvajol and coll. [59] studied the doping of individual double-walled carbon nanotubes with molten-iodine, on the basis of the already mentioned selective Raman responses arising from either inner or outer tubes in this case. As for bromine [57], only the signals relevant to outer tubes were found to be affected by I-doping, indicating location of iodine at the outer surface. This result contrasts with the filling of the central cavity reported for some SWNTs under similar conditions [19]. The presence of I_n^- species was again inferred from some low frequency features appearing in the Raman spectra, providing an unambiguous evidence of holes injection into the carbon host-lattice electronic structure. Charge transfer should consequently occur from the outer wall only, in compliance with the blue shift observed for the sole outer tubes TM.

2.2.2. Lewis acids

Chlorides: A combination with $FeCl_3$ is listed among the very first intercalation attempts reported from MWNTs, for some reasons already exposed in the preceding part. Hence, intercalation of $FeCl_3$ into MWNTs of arc-discharge origin, believed to be of the scroll-type, was reported in a series of papers by Mordkovich et al. [60-62]. In their analysis, abstraction was made of the particular bundled arrangement of the tubes, present in the sample used, which may also be responsible for some chloride fixation. Thus, the XRD

signature matched that obtained from the homologous first stage GIC, indicating some structural similarity with the latter, which was partly confirmed by direct TEM observation of the location of intercalate layers between the curved graphene sheets. More puzzling is the observation of a pearl necklace-like overall morphology, corresponding to a successive alternation of intercalated and non-intercalated zones. The doping scheme is unexpectedly non-homogeneous, for some unclear reason, since a true scroll-like arrangement should allow diffusion down the whole interlayer channel. In a subsequent work [63, 64] devoted to the comparison of the reactivity of either scroll-like or Russian doll-like MWNTs batches, the same author showed that the latest type is, as expected, inert in regard to intercalation or breaks into intercalated graphite nanoflakes when the walls thickness is too small. This effect has likely to be related to the fragilization generated by the higher strain present within the curved outer shells of thinner tubes. The successful intercalation of some other metal chlorides, using a chlorine atmosphere, was also briefly mentioned, showing a dilation of the interlayer separation.

Transport measurements [65, 66] on $FeCl_3$-intercalated MWNTs revealed the existence of distinct regimes, separated by a maximum in conductivity marking a temperature limit for quantum effects on transport.

Fluorides: Due to the presence of a strongly electronegative ligand, such oxidizing agents stand as ideal candidates liable to give birth to a strong interaction with a carbon matrix. They are already well known to yield charge transfer intercalation compounds with different allotropic forms of carbon like graphite, or still fullerenes, as will be seen in the next part. WF_6 was first chosen as such a prototype of electron acceptor [67], owing to its ability to readily intercalate graphite in the presence of gaseous fluorine. Based on relative intensities calculations, stemming from a structural model mirroring the homologous GIC along the layers stacking direction, a good adequacy of the diffraction data with a staging phenomenon limited to the surface could be established. Intercalation happened to be only partial, as usual in this case may one be tempted to say, leaving large parts of the sample unaffected by the reaction. This was attributed to a limited lateral and core diffusion of the dopant, within restricted perimeters where wall disruptions were present.

Extending the previous work to the study of the electronic properties of some fluorides-intercalated MWNTs phases, using ESR spectroscopy [68], the same group observed the creation of localized unpaired spins on the host carbon frame. This was assigned to a charge transfer process resulting from the formation of both interplanar and surface fluoroanions, via a F_2-assisted mechanism. Formal identification, by ^{19}F NMR spectroscopy, of the BF_4^- species gave complementary convincing evidence of the formation of such anions.

2.3. Perspectives

Owing to the widespread range of interest in which carbon nanotubes are expected to lead to promising technological developments on a short term, concepts related with the valorisation of their intercalated derivatives have not been long to emerge. Again focusing on the sole p-type doping case, it may be tempting to close this chapter with a look across some recent concrete outcomes in the matter.

While it seems clear that the bundle configuration may not be optimal regarding miniaturization, most of the potential applications under the form of optically active materials, chemical sensors, or nanoelectronic devices, would moreover require bulk separation of the metallic from the semi-conducting tubes. Consequently, sorting necessitates preliminary individualization. Considering such a necessity to operate with isolated tubular entities, Lee and coll. [23] suggested to retain the exfoliation process that accompanies intercalation/de-

intercalation cycles with nitric acid molecules as an efficient means of individualizing nanotubes from bundles. Though the process may suffer from side reactions leading to the grafting of functionalities to the sidewall, subsequent annealing in view of their elimination could be envisaged.

An enrichment process based on the formation of charge transfer complexes with bromine was proposed [69], which may pave the way toward efficient separative methods. Indeed, the selective chemical attack of metallic tubes, as compared to that of semi-conducting ones, confers to the former a higher specific gravity, and could serve for their separation by high-speed centrifugation. The higher chemical reactivity of strained bonds also allows a diameter selective attack of the thinner tubes by some oxidizers. Several etching chemical treatments with H_2SO_4/HNO_3 mixtures have thus been developed [70, 71], which yield a final product enriched with large diameter SWNTs. Several authors have afterward outlined the also metallicity-dependent character of such a destructive process. Selective removal of small diameter metallic SWNTs has been achieved [72-74] using the NO_2^+ cation as destroying intercalant, employing as sources either NO_2SbF_6 or the former sulfo-nitric mixture, which also produces the nitronium ion. The observed effect was imputed to a more available charge density at the Fermi level from metallic SWNTs, which therefore interact more strongly with the cation.

The recent elaboration of endohedral charge transfer complexes [49, 53] offers a new opportunity to achieve tailoring of the electronic properties of carbon nanotubes, and therefore to put an end to the preceding problematic. Not only has the encapsulation of organic molecules proved to give highly stable edifices, owing to the protective action of the outer wall in regard to oxygen or moisture and to a not energetically favourable de-encapsulation, but it may also allow a more flexible tuning of the carriers concentration, which has always been a major difficulty with any other physico-chemical doping technique. It may then be at the origin of imminent decisive progress in the practical realization of components for molecular electronics.

It is now well established that their overall geometrical aspect, excellent thermal stability and adequate electronic properties can make carbon nanotubes remarkably stable field electron emitters under low operating voltage, producing high current densities with low fluctuations. It has then become common sense to infer that change in their electronic structure should affect their field emission properties. Though the latest happen to arise from a subtle balance in the influences exerted by several parameters [75], it is to be feared that lowering the Fermi level via p-type doping, i.e. increasing the work function, would not benefit the field emission performances of carbon nanotubes. A naïve analogy with the observed improvement of the latter [75] upon substitutional n-doping of tubes with N atoms, would tend to confirm the preceding pessimistic forecast in regard to the usefulness of any kind of hole-doped carbon nanostructures in field emission devices.

Nanocomposites might be the field par excellence in which the compact rope configuration could be interesting . Thus, the processing of SWNTs in 100% sulfuric acid or oleum yields acid intercalated ropes, whose alignment is promoted via electrostatic interactions [37]. Extruding such a phase was shown to produce highly oriented continuous macroscopic SWNTs fibers [38], which may be high quality reinforcing agents for polymer or ceramic matrices.

Discontinuities in the MWNTs morphology, and their resulting inhomogeneous doping, make their electronic properties less easy to exploit, and their interest might more surely reside in their particular geometrical aspect, for instance. Indeed, MWNTs can allow the confinement of a chemical reaction within the limits of their curved interlayer space. A ligand exchange-like reaction, involving fluoride-intercalated MWNTs, has recently proved [76] that such edifices can be efficient templates for the production of heteroatomic nanoparticules.

According to the same conceptual approach, polymerisation reactions may also be conducted in the interlayer space and thus yield sandwich nanocomposites.

The present list would be far from exhaustive without quoting some other clear aims pursued, keeping in mind that perspectives in the matter still remain somewhat speculative. Hence, according to standard models, the upper temperature threshold characterizing a superconducting state varies as $\exp(-1/N(E_F))$, with $N(E_F)$ being the DOS at the Fermi energy. The fluctuation induced in the Fermi level upon doping may bring the latter in coincidence with a van Hove singularity and then produce high temperature superconducting materials. Such a modulation is not the apanage of the chemical hole-doping methods, however. From an other point of view, one may also imagine that the strengthening of the carbon-carbon bond, which follows diminution of the internal screening after electron removal, systematically makes p-doped SWNTs ropes interesting candidates for the reinforcement of composites. Furthermore, it may not be surprising to see research trends emerge relating to the electrochemistry of SWNTs salts. An outlook in the matter resides in the use of an oxidized lattice of nanotubes as an electrochemically active part of a rechargeable battery. The possibilities offered are probably best exemplified through encapsulated acceptors. Indeed, the discharge process associated to such edifices is frozen at the level of an intermediate reduction of the preliminary oxidized carbon wall. The carbon cage thus plays the role of a buffer redox state, from which correct cyclability can be expected.

3. THE P-TYPE DOPING OF FULLERENES

Due to their overall spherical aspect, fullerenes molecules in the condensed state very often adopt the universal compact arrangements governing the self-organization of rigid spheres. This trend is amplified by effective rotational molecular motion at ambient temperature, which raises the apparent symmetry of the plastic crystals that they form. Regarding intercalation chemistry, the geometrical criteria necessary for accommodation of guest species are fulfilled through the presence of large interstitial cavities throughout the carbon matrices. The lowered dimensionality, arising from a now absent tight binding in the space directions, also makes fullerites true Van der Waals solids, which facilitates lattice distortion and the creation of more available space if accommodation of large intercalant species is required.

However, the amphoteric character of fullerenes is far less pronounced than for the preceding carbon allotropes reviewed, and their overall chemical reactivity is summarized in terms of a strongly electron-deficient character. Similarly, both the high ionisation energy values measured or the often high electrochemical oxidation potentials in solution reported clearly reflect the reluctant trend to oxidation of isolated molecules, a consequence naturally imputable to their electronic structure, which will equivalently mean great hindrance in injecting holes into the small width π-derived bands, arising from the weak intersite overlap of molecular levels (Fig. 8), when the carbon network is concerned as a whole. Consequently, the oxidative doping of fullerenes crystals turns out to be difficult and necessitates the use of strong oxidizing agents. On such grounds, the synthesis of fullerenium salts has remained a marginal event in fullerene chemistry, so far.

The following paragraphs give a brief summary concerning some essential characterization methods that have commonly been employed in the diagnostic of the oxidation states of fullerenes molecules, either isolated or within crystals. The range of techniques employed for the study of anionic derivatives (fullerides) has been covered in an excellent and impressively detailed review article by Reed and Bolskar [3]. We will limit the forthcoming description to a concise evocation of those that have been extended to the study

of fullerenic cations and which also allow a direct comparison to the results previously exposed for SWNTs. [60]fullerene will be used as reference for illustration, each time.

Due to the high sensitivity of Raman scattering toward changes in both the symmetry and electronic structure, this technique has given some clues for the understanding of fullerenes redox chemistry in solution and in the condensed state. In the case of C_{60}, measurements on undoped crystals show a splitting into height H_g and two A_g modes, as predicted by group theory for icosahedral symmetry. Those conserving I_h symmetry, associated with centrosymmetric sphere breathing or antisymmetric and out of phase stretching of 6-6 and 6-5 bonds, denoted $A_g(1)$ and $A_g(2)$ respectively, give the most prominent contributions (6-6 and 6-5 refer to hexagone-hexagone and hexagone-pentagone shared carbon-carbon bonds). For some reasons already invoked in the first part, Raman responses can constitute an efficient probe of the charge state at a carbon site. In the case of [60]fullerides anions, the so-called pentagonal pinch mode $A_g(2)$ at ~1469 cm^{-1} was indeed shown to experience a characteristic frequency red shift, by 6-7 cm^{-1} per extra-charge transferred to the C_{60} molecule, independently of the doping cation. It seems that the similar scale, with opposite sign, also applies to positively charged fullerene clusters, as discussed in the following. Similar effects were also reported from the IR active-modes.

The Vis-NIR absorption spectrum of fullerenes is dominated by π-π^* transitions. Changes in the occupation of the electronic levels, accompanying charge transfer, generate new optically allowed transitions, reflected in turn by new features in the absorption spectrum. These have been widely used to characterize either fulleride anions or, to a lesser extent, some fullerenium radical carbocations, in a transient state most of the time. A schematic illustration of the mechanisms involved is proposed in figure 8, with reference to the C_{60} diagram of energy levels. Such modifications can also reflect the energy splitting, upon charging, of some initially partially degenerate orbitals.

3.1. Halogens

I_2: While the more electronegative F, Cl and Br elements all give addition reactions, iodine is the only halogen that does not covalently bond to a fullerene cage. Iodine is known to not insert into the graphite lattice for some incompatibilities of geometrical origin, which are presently raised in the case of a 0D network, and it is also known to yield highly conductive charge transfer compounds with some polycyclic aromatic hydrocarbons. Whether some kind of such ionic charging might also be expected from a similar combination with fullerenes may be intuitively assessed through a naïve comparative picture of the electron affinity of the iodine atom (3.06 eV) with the first ionization potential of the C_{60} molecule (7.6 eV), for instance, which seems to preclude the opportunity of an oxidative doping process. Nevertheless, this does not prevent the intercalation of iodine into the [60]fullerene lattice to be easily carried out [77-79] from a gas-phase reaction in sealed evacuated tubes, over the 100-300°C temperature range. An alternating sequence of carbon and iodine layers is obtained, described either in a base-centered orthorhombic mode for a composition $C_{60}I_2$ [78, 79], or possessing hexagonal symmetry when approaching the $C_{60}(I_2)_2$ saturation composition [77]. Both phases, similar in regard to their basic features, admit possible departure from the ideal stoichiometry.

The closest I-I distance identified is compatible with molecular iodine accommodated into the interstitial channels of the carbon host lattice, and indeed confirms that the process is apparently non oxidative. The compounds behave as dielectrics in standard conditions [77-80], also suggesting that no charge transfer occurs. Mössbauer, Raman and XANES spectroscopies [81-85] confirmed the presence of neutral iodine molecules in the lattice and ruled out the formation of anionic species and thus, the existence of a formal electron exchange. The

deviation observed from the intramolecular bond length value in elemental di-iodine is usually an indicator of minor charging effects, corresponding here to an $I_2^{\delta+}$ state, in other words, partial electron transfer rather occurs from iodine to C_{60}. So, to the question whether iodine induces or not the true hole-doping of C_{60} crystals, the answer is definitely no.

A body-centered tetragonal unit cell, with both the principal axis of the rugby-ball shaped molecule and that of the halogen dimer oriented along the c axis, was proposed [79] for a $C_{70}I_2$ compound, obtained in similar conditions. The existence of a higher doping level $C_{70}I_4$, with an unresolved crystal structure, was also inferred. There is no reason for the electronic properties of iodine-doped [70]fullerene samples to be fundamentally different from the previous case.

Interhalogen compounds: an alternative to increase the oxidizing strength of the presently examined category of dopants, while avoiding covalent addition to carbon, is to substitute one of the atoms of the di-iodine molecule with one or more electronegative halogen atoms, which at the same time turns down the natural bonding affinity of the latest for the carbon frame. Thus, the synthesis of an $(IBr)_3C_{60}$ phase, with a likely base-centered orthorhombic structure recalling that of iodine-doped samples, was reported [88].

It exhibits some kind of ferromagnetic ordering [86, 87] below 30 K, to be correlated with a measured concentration of 0.2 spin/C_{60}, that probably resulted from the creation of holes according to the authors. The influence exerted on the initial electronic states by the presence of this electrophilic species was also illustrated by a quite different magnitude of the ^{13}C-NMR spin-lattice relaxation time [89], as compared to that measured for C_{60} or iodine-intercalated C_{60} samples. The appearance of a metallic character was discussed in terms of band hybridization rather than true charge transfer, however.

3.2. Lewis acids

We previously evoked this class of reagents as part of the standard combinations entering the earlier studies on the intercalation chemistry of graphite, and there is general acknowledgement about their high electron withdrawing character in regard to graphene sheets. These are consequently excellent candidates likely to generate fullerenium carbocations.

Transition metal halides: A hexagonal phase, exhibiting a notable cell expansion in regard to the one initially characterizing the host lattice, was reported [90] following the reaction of [60]fullerene with MoF_6, in the absence of a gaseous fluorine atmosphere. The provisional stoichiometric ratio established from weight uptake was 6:1, but probably suffered from adsorption/condensation effects. IR, ESR and ^{19}F NMR spectroscopies all converged in the direction of MoF_5 being the dominant intercalated species. Hence, reduction of the metal halide implies oxidation of the carbon network, according schematically to $2\ MoF_6 + C \rightarrow MoF_5 + C^+ + MoF_7^-$. Indeed, the IR signature of the fluoromolybdate anions was seemingly recorded. Partial fluorination of carbon was also mentioned, which could also account for reduction of part of the metal fluoride. The same team further extended the study using various tetra to hexavalent fluorides of different transition metals [91, 92], and concluded in similar reaction patterns, though the results suffered from ill-defined stoichiometries and from the absence of advanced structural characterization, in spite of the sometimes good apparent crystalline quality of the intercalation compounds thus prepared. Specific problems encountered in the search of a more efficiently controlled synthesis mode were outlined [93] and plausibly involve a moderate stability of the doped phases in such harsh conditions.

Interestingly, the room temperature electrical conductivity of some samples after such redox doping processes was found to increase by several orders of magnitude [91].

Halides of post-transition elements: Datars et al. succeeded in the intercalation of AsF_5 into the [60]fullerene lattice [94], from an elegant low temperature synthesis route in solution, likely to improve the homogeneity of the final sample, by employing liquid SO_2 as solvent. The nominal composition established by gravimetry was in the vicinity of two intercalant species per C_{60}. The corresponding diffraction pattern was indexed on the basis of a body-centered tetragonal unit cell. In a subsequent report [95], the same authors identified unambiguously the chemical nature of the intercalated species. From very close analogies with the IR and ^{19}F NMR spectra of reference fluoroarseniate compounds, they concluded in the exclusive presence of the AsF_6^- anion and explained its formation according to $3\ AsF_5 + 2\ e^- \rightarrow 2\ AsF_6^- + AsF_3$, under the assumption that electrons were removed from the fullerene clusters. Given the ionic radii ratio, it is likely that the structural architecture should lie on the large fullerene molecule acting as the main building block of the body-centered cell previously identified. The somewhat notable size of the associated fluoroanion suggests that the latter should then be distributed over the largest vacancies available inside a distorted packed array of fullerene clusters. A geometrical analysis of the size of the various interstices present in such a matrix was detailed in a paper by Datars and coll. [96] who suggested tetrahedral coordination for the fluoroanion. However their limit packing rules were established by assigning the C_{60} cluster an outer radius corresponding to the σ-bonded inner frame, whereas the effective crystal radius of a C_{60} sphere is in fact much closer to its Van der Waals radius, as that derived from the equilibrium distance in the pristine material (0.5 nm). Taking into account the outward extension of the π cloud creates a mismatch between the respective sizes of the intercalant and tetrahedral interstices. Therefore, a more likely configuration may consist of oriented AsF_6^- species lying at the center of each face, though this would imply deviation from the experimental 1.9:1 stoichiometric ratio, normalized to the fullerene molecule. Somehow, we may note that the latter was determined from weight uptake assuming an $(AsF_5)_xC_{60}$ formulation, and was never corrected after proper identification of the anionic nature of the intercalant. Taking into account one more F atom entering the mass difference, we may then reformulate the composition as $(AsF_6)_{1.7}C_{60}$, which is closer to x = 1.5 than to x = 2, and within experimental error, probably compatible with the structural hypothesis proposed. A recent high field ^{19}F NMR characterization [98], offering good spectral resolution, showed two distinct features suggesting that fluoroanions are located in two different interstitial sites, which is not in contradiction with the previous hypothesis. At room temperature, narrow signals, characteristic of efficient dipole-dipole interaction averaging, showed that fluorinated intercalants undergo rapid reorientation, whereas a broad and asymmetric ^{13}C line indicated that the [60]fullerene frame is rigid [97]. A lattice dynamics study [98] did not reveal any hindrance toward free rotation of the fluoroanion down to at least 67 K.

Owing to the successful intercalation of AsF_6^-, similar reaction paths were thereafter attempted [99] from other hexafluoroanions of group V elements (M = Sb and P), using NO_2MF_6 salts as precursors, in the 2:1 molar ratio with respect to C_{60}. The non-detection of N-O residual features coupled to the persistence of M-F bands, during IR analysis of the solids obtained, as well as the formation of colored NO_2 in the course of reactions, both gave qualitative evidence that the nitronium ion can efficiently oxidize the carbon cluster. A properly speaking charge transfer intercalation compound is thus formed upon association with the counter-fluoroanion for charge neutralisation. The reversible character of such an incorporation of the MF_6^- anions into the fullerene lattice, outlining the pertinence of the terminology employed, was illustrated from the recovery of the IR spectrum of the initial fullerite after heat treatment under vacuum. Hence, since in no way does the initial molar ratio

define the final stoichiometry of the intercalated phase, a presumptive $(SbF_6)_{\sim 2}C_{60}$ phase was obtained, on which structural information remains quite limited. Similar conclusions, as compared to the homologous As-based phase, were drawn from ^{19}F and ^{13}C NMR characterization [97, 98], regarding molecular motion at room temperature and chemical environment. A molecular dynamics study showed that freezing of molecular reorientation, probably induced by steric hindrance given the larger size of the present hexafluoroanion, occurs at different temperature thresholds upon cooling [98], which seemingly corroborates the hypothesis of different interstitial sites.

^{13}C NMR measurements [100] on the analogously obtained $(PF_6)_{\sim 2}C_{60}$ derivative revealed freely rotating fullerene molecules at room temperature, whereas the ^{31}P spectrum exhibited two well distinct components, of possible structural origin, though not formally explained.

Shifts in the positions of the IR active modes of the C_{60} molecule, upon doping with MF_6^- (M = P, As, Sb) species, were qualitatively correlated to the modification of its electronic states [99]. A more quantitative subsequent analysis was provided on the basis of the blue shift experienced by the Raman active $A_g(2)$ mode [101]. It was proposed that its amplitude indeed correlated with a charge transfer amount equivalent to C_{60}^{2+}, in this case. This raises the question of the ground state spin configuration for such a carbocation. ^{13}C NMR spectroscopy revealed a significant reduction of the spin-lattice relaxation times in such samples, in comparison to that relative to the pristine fullerene lattice, which suggested the presence of localized paramagnetic centers [97]. Magnetic susceptibility measurements [100] confirmed the paramagnetic behavior suspected, but the low Curie constant values determined were in favour of the adoption by the cations of a diamagnetic singlet configuration. The origin of the paramagnetic contribution was attributed to dangling bonds or structural defects, created in the course of the oxidation process.

The p-type doping, using halogenated Lewis acids, of C_{60} samples either under the form of pressed powders or of films, seems to be systematically accompanied by a severe drop of the electrical resistance at room temperature. Samples doped with AsF_5, $SbCl_5$ or $InCl_3$ were shown to exhibit typical semiconducting behaviors [102-104], with temperature dependent resistive features following variation laws of the Arrhenius type. Sudden variations at low temperatures were tentatively interpreted in terms of possible structural transitions or complex electron transition patterns. A concomitant variation of both the electrical and optical properties of C_{60} films was also reported [105] upon doping with gaseous SbF_5. The increased room temperature conductivity was found to correlate with the quenching of some optical absorption features apparently involving the HOMO-derived levels, suggesting electron depletion of the fullerene lattice valence band.

3.3. Some “exotic” fullerenium salts

Previously described in the above section from NO_2MF_6 type reagents, the cation-assisted method for generating positively ionized fullerene molecules, according schematically to $C_n + A^+ + B^- \rightarrow <C_n^+ + B^-> + A$, seems to have been published for the first time ten years ago [106]. As emphasized by its initiators, its success lies less in the oxidizing properties of the cationic charge transfer mediator, than in the extremely low nucleophilicity of the counter-anion initially present or of its ligands, which prevents subsequent addition to take place on the charged carbon cage. The same holds true regarding some moities entering the reduced electron acceptor. Thus, brominated derivatives of triarylaminium radical cations have proved effective oxidants in regard to [76] and [60]fullerenes, yielding, in combination with the inert hexahalogenated carborane anions ($CB_{11}H_6X_6^-$), C_{76}^+ and C_{60}^+ radical cations in solution, from which some rather unconventional crystalline ionic salts have been isolated [106, 107].

ESR spectroscopy revealed characteristic doublet spin states, with g values close to the free electron value, in parallel with the consequent evolution expected in the NIR absorption spectrum.

3.4. Prospects

Obtaining fullerenium salts still remains an open challenge that may be more likely taken up with high mass fullerenes, since the evolution of the energy required for positively or negatively charging a fullerene molecule inversely depends on the cluster size, according to a satisfying electrostatic model involving a macroscopic-like description of their molecular capacitance [108]. Up to date, an experimental hiatus in this field must be faced, however, due to the still limited availability of fullerenes beyond C_{70}.

One may expect the chemical hole-doping of fullerene materials to arouse interest in fields similar to those previously concerned by their chemical n-type doping. Thus, attention used to be focused essentially on electrical, magnetic and optical properties. Though a real appealing potency in the matter for hole-doped fullerenes remains to be practically demonstrated, it may be worth to here recall that the conductivity of an AsF_5-GIC was found to approach that of metallic copper, an experimental fact pointing out the underlying interest of further exploration in the synthesis and characterization of other p-doped carbon allotropes.

In comparison to doping with electron donors, doping with electron acceptors offers a comparatively efficient way to tune the Fermi level in fullerene-derived condensed phases. Therefore, one essential motivation for further developments in their intercalation chemistry with acceptors may reside in the search for high temperature superconductors. Indeed, in the case of C_{60} intercalation compounds, a superconducting state can follow electron injection into the band derived from the threefold degenerate LUMO of the isolated cluster (Fig. 8). Hole-doping of the lower HOMO-derived filled band is of particular interest, as one might expect a similar state to appear, with T_c potentially scaling up in the framework of BCS theory, owing to the higher density of electronic states at the Fermi level which results from the higher orbital degeneracy (Fig. 8). Account may also be taken of other arguments in favor of an increased electron-phonon coupling strength in such crystals, likely to further raise T_c.

Beside superconductivity and regarding (nano)electronics, Datars and coworkers [97, 98] suggested the realization of p-n junctions based on antagonistically doped fullerene crystals sides. Further extrapolation of the present concept beyond electronic components may naturally lead one to consider a fundamental application of such a junction as the heart of a photovoltaic cell. Concrete experimentation would be necessary to evaluate the performances regarding the production of light-stimulated electrons, in comparison to conventional silicon, but one may anticipate that, due to their excellent ability to be processed as thin films, subsequently doped fullerene materials might easily enter into the newly developed multilayer designs of such semiconductor devices.

To address the question whether some promising magnetic properties are to be expected or not, one may, in the first place, refer to the direct correspondence between the π MOs of C_{60} and the spherical harmonics issued from a simplified treatment of the relevant π system in terms of free electrons on a sphere. Introduction of the icosahedral perturbation splits the former l-dependent functions, l being an azimuthal quantum number, into the irreducible components of the I_h point group. The $l = 5$ level is thus partially decomposed into the degenerate HOMO and LUMO subsets of figure 8, from which values of the total angular momentum quantum number J can be calculated for spin states of the C_{60} molecular ions, from application of Hund's rule [109]. Due to the higher degeneracy of the electron-donor HOMO levels, as compared to the electron-acceptor LUMO levels, the largest J values are then predicted for those non-closed shell configurations resulting from the positive ionization

of the cluster. Accordingly, the largest magnetic moments in the ground state should occur for the +2 (J = 4) and +3 (J = 9/2) molecular ions, as long as reasonable charge states are considered. This raises hope regarding future progress in acceptor-doped C_{60} compounds as permanent magnets.

Intercalation and electrochemical energy storage have been closely related since the emergence of second and third generation rechargeable batteries. A prospective investigation of the use of an oxidized fullerene matrix as cathode material in lithium batteries was reported [93], but depicted too limited performances for practical applications to be envisaged, however. A mechanism involving the formation of an intercalated lithium fluorometallate complex and the reversible reduction of the carbon molecules was proposed.

As a final comment, one may also underline that the potential interest of fullerene-based intercalation compounds regarding technological applications may be increased by the facile processing of the carbonaceous precursor as much under the form of coatings or thin films as of bulk crystals or powders, an advantage inherent to its molecular nature. One of the main problem to deal with remains of course the air sensitivity of derivatives involving fullerene molecules in a non electrically neutral charge state, regardless of their anionic or cationic nature.

References and Notes

1. L. Duclaux, *Carbon* 40, 1751 **(2002)**

2. M. Rosseinski, *Chem. Mat.* 10 (10), 2665 **(1998)**

3. C. A. Reed, R. D. Bolskar, *Chem. Rev.* 100, 1075 **(2000)**

4. J. E. Fisher, *Acc. Chem. Res.* 35, 1079 **(2002)**

5. R. Saito, G. Dresselhaus, M. S. Dresselhaus, *Phys. Rev. B* 61 (4), 2981 **(2000)**

6. H. Kataura, Y. Kumazawa, Y. Maniwa, I. Umezu, S. Suzuki, Y. Ohtsuka, Y. Achiba, *Synth. Met.* 103, 2555 **(1999)**

7. N. Minami, S. Kazaoui, R. Jacquemin, H. Yamawaki, K. Aoki, H. Kataura, Y. Achiba, *Synth. Met.* 116, 405 **(2001)**

8. A. Jorio, M. A. Pimenta, A. G. Souza Filho, R. Saito, G. Dresselhaus, M. S. Dresselhaus, *New J. Phys.* 5, 139 **(2003)**

9. R. S. Lee, H. J. Kim, J. E. Fisher, A. Thess, R. E. smalley, *Nature* 388, 255 **(1997)**

10. A. M. Rao, P. C. Eklund, S. Bandow, A. Thess, R. E. Smalley, *Nature* 388, 257 **(1997)**

11. A. M. Rao, S. Bandow, E. Richter, P. C. Eklund, *Thin Solid Films* 331, 141 **(1998)**

12. P. Petit, C. Mathis, C. Journet, P. Bernier, *Chem. Phys. Lett.* 305, 370 **(1999)**

13. S. Kazaoui, N. Minami, R. Jacquemin, H. Kataura, Y. Achiba, *Phys. Rev. B* 60 (19), 13339 **(1999)**

14. R. Jacquemin, S. Kazaoui, D. Yu, A. Hassanien, N. Minami, H. Kataura, Y. Achiba, *Synth. Met.* 115, 283 **(2000)**

15. S.-H. Jhi, S. G. Louie, M. L. Cohen, *Solid State Commun.* 123, 495 **(2002)**

16. L. Grigorian, K. A. Williams, S. Fang, G. U. Sumanasekera, A. L. Loper, E. C. Dickey, S. J. Pennycook, P. C. Eklund, *Phys. Rev. Lett.* 80 (25), 5560 **(1998)**

17. D. E. Sklovsky, V. A. Nalimova, J. E. Fisher, *Mol. Materials* 13, 59 **(2000)**

18. X. Fan, E. C. Dickey, P. C. Eklund, K. A. Williams, L. Grigorian, R. Buczko, S. T. Pantelides, S. J. Pennycook, *Phys. Rev. Lett.* 84 (20), 4621 **(2000)**

19. U. D. Venkateswaran, E. A. Brandsen, M. E. Katakowski, A. Harutyunyan, G. Chen, A. L. Loper, P. C. Eklund, *Phys. Rev. B* 65, 054102-1 **(2002)**

20. N. Bendiab, R. Almairac, S. Rols, R. Aznar, J.-L. Sauvajol, *Phys. Rev. B* 69, 195415-1 **(2004)**

21. C. Bower, A. Kleinhammes, Y. Wu, O. Zhou, *Chem. Phys. Lett.* 288, 481 **(1998)**

22. K. H. An, K. K. Jeon, J.-M. Moon, S. J. Eum, C. W. Yang, G.-S. Park, Y. H. Lee, *Synth. Met.* 140, 1 **(2004)**

23. H. J. Kim, K. K. Jeon, K. H. An, C. Kim, J. G. Heo, S. C. Lim, D. J. Bae, Y. H. Lee, *Adv. Mat.* 15 (20), 1757 **(2003)**

24. F. Hennrich, R. Wellmann, S. Malik, S. Lebedkin, M. M. Kappes, *Phys. Chem. Chem. Phys.* 5, 178 **(2003)**

25. M. E. Itkis, S. Niyogi, M. E. Meng, M. A. Hamon, H. Hu, R. C. Haddon, *Nanolett.* 2 (2), 155 **(2002)**

26. M. T. Martinez, M. A. Callejas, A. M. Benito, M. Cochet, T. Seeger, A. Anson, J. Schreiber, C. Gordon, C. Marhic, O. Chauvet, J. L. G. Fierro, W. K. Maser, *Carbon* 41, 2247 **(2003)**

27. M. T. Martinez, M. A. Callejas, A. M. Benito, M. Cochet, T. Seeger, A. Anson, J. Schreiber, C. Gordon, C. Marhic, O. Chauvet, J. L. G. Fierro, W. K. Maser, *Nanotechnol.* 14, 691 **(2003)**

28. R. Graupner, J. Abraham, A. Vencelova, T. Seyller, F. Hennrich, M. M. Kappes, A. Hirsch, L. Ley, *Phys. Chem. Chem. Phys.* 5, 5472 **(2003)**

29. W. Zhou, J. Vavro, N. M. Nemes, J. E. Fisher, F. Borondics, K. Kamaras, D. B. Tanner, *Phys. Rev. B* 71, 205423 **(2005)**

30. P. Szroeder, W. Marciniak, F. Rozploch, *Karbo* 6, 168 (2002)

31. G. U. Sumanasekera, J. L. Allen, S. L. Fang, A. L. Loper, A. M. Rao, P. C. Eklund, *J. Phys. Chem. B* 103 (21), 4292 **(1999)**

32. G. Sumanasekera, J. Allen, P. Eklund, *Mol. Cryst. Liq. Cryst.* 340, 535 **(2000)**

33. S. Lefrant, M. Baibarac, I. Baltog, J. Y. Mevellec, L. Mihut, O. Chauvet, *Synth. Met.* 144, 133 **(2004)**

34. I. Baltog, S. Lefrant, M. Baibarac, L. Mihut, N. Preda, T. Velula, *Rom. J. Phys.* 49 (9-10), 751 **(2004)**

35. P. Corio, P. S. Santos, V. W. Brar, G. G. Samsonidze, S. G. Chou, M. S. Dresselhaus, *Chem. Phys. Lett.* 370, 675 **(2003)**

36. S. Ramesh, L. M. Ericson, V. A. Davis, R. K. Saini, C. Kittrell, M. Pasquali, W. E. Billups, W. W. Adams, R. H. Hauge, R. E. Smalley, *J. Phys. Chem. B* 108 (26), 8794 **(2004)**

37. V. A. Davis, L. M. Ericson, A. N. G. Parra-Vasquez, H. Fan, Y. Wang, V. Prieto, J. A. Longoria, S. Ramesh, R. K. Saini, C. Kittrell, W. E. Billups, W. W. Adams, R. H. Hauge, R. E. Smalley, M. Pasquali, *Macromolecules* 37 (1), 154 **(2004)**

38. L. M. Ericson, H. Fan, H. Peng, V. A. Davis, W. Zhou, J. Sulpizio, Y. Wang, R. Booker, J. Vavro, C. Guthy, A. N. G. Parra-Vasquez, M. J. Kim, S. Ramesh, R. K. Saini, C. Kittrell, G. Lavin, H. Schmidt, W. W. Adams, W. E. Billups, M. Pasquali, W.-F. Hwang, R. H. Hauge, J. E. Fisher, R. E. Smalley, *Science* 305, 1447 **(2004)**

39. P. Corio, A. Jorio, N. Demir, M. S. Dresselhaus, *Chem. Phys. Lett.* 392, 396 **(2004)**

40. S. Kazaoui, N. Minami, N. Matsuda, H. Kataura, Y. Achiba, *Appl. Phys. Lett.* 78 (22), 3433 **(2001)**

41. V. Skakalova, A. B. Kaiser, U. Dettlaff-Weglikowska, K. Hrncarikova, S. Roth, *J. phys. Chem. B* 109 (15), 7174 **(2005)**

42. U. Dettlaff-Weglikowska, V. Skakalova, R. Graupner, S. H. Jhang, B. H. Kim, H. J. Lee, L. Ley, Y. W. Park, S. Berber, D. Tomanek, S. Roth, *J. Am. Chem. Soc.* 127 (14), 5125 **(2005)**

43. X. Liu, T. Pichler, M. Knupfer, J. Fink, H. Kataura, *Phys. Rev. B* 70, 205405 **(2004)**

44. A. Kukovecz, T. Pichler, R. Pfeiffer, H. Kuzmany, *Chem. Commun.* 1730 **(2002)**

45. A. Kukovecz, T. Pichler, R. Pfeiffer, C. Kramberger, H. Kuzmany, *Phys. Chem. Chem. Phys.* 5, 582 **(2003)**

46. L. Kavan, M. Kalbac, M. Zukalova, L. Dunsch, *J. Phys. Chem. B* 109 (42), 19613 **(2005)**

47. S. Kazaoui, N. Minami, H. Kataura, Y. Achiba, *Synth. Met.* 121, 1201 **(2001)**

48. S. Kazaoui, Y. Guo, W. Zhu, Y. Kim, N. Minami, *Synth. Met.* 135-136, 753 **(2003)**

49. T. Takenobu, T. Takano, M. Shiraishi, Y. Murakami, M. Ata, H. Kataura, Y. Achiba, Y. Iwasa, *Nature materials* 2, 683 **(2003)**

50. J. Lu, S. Nagase, D. Yu, H. Ye, R. Han, Z. Gao, S. Zhang, L. Peng, *Phys. Rev. Lett.* 93 (11), 116804-1 **(2004)**

51. W. Z. Liang, J. Yang, J. Sun, *Appl. Phys. Lett.* 86, 223113 **(2005)**

52. V. Meunier, B. G. Sumpter, *J. Chem. Phys.* 123, 024705-1 **(2005)**

53. M. Shiraishi, S. Swaraj, T. Takenobu, Y. Iwasa, M. Ata, W. E. S. Unger, *Phys. Rev. B* 71, 125419-1 **(2005)**

54. Ph. Lambin, A. Loiseau, C. Culot, L. P. Biro, *Carbon* 40, 1635 **(2002)**

55. A. Hamwi, H. Alvergnat, S. Bonnamy, F. Beguin, *Carbon* 35 (6), 723 **(1997)**

56. Z.-X. Jin, G. Q. Xu, S. H. Goh, *Carbon* 38, 1135 **(2000)**

57. G. Chen, S. Bandow, E. R. Margine, C. Nisoli, A. N. Kolmogorov, V. H. Crespi, R. Gupta, G. U. Sumanasekera, S. Ijima, P. C. Eklund, *Phys. Rev. Lett.* 90 (25), 257403-1 **(2003)**

58. W. Zhou, S. Xie, L. Sun, D. Tang, Y. Li, Z. Liu, L. Ci, X. Zou, G. Wang, P. Tan, X. Dong, B. Xu, B. Zhao, *Appl. Phys. Lett.* 80 (14), 2553 **(2002)**

59. J. Cambedouzou, J. L. Sauvajol, A. Rahmani, E. Flahaut, A. Peigney, C. Laurent, *Phys. Rev. B* 69, 235422 **(2004)**

60. V. Z. Mordkovich, M. Baxendale, S. Yoshimura, R. P. H. Chang, *Carbon* 34, 1301 **(1996)**

61. V. Z. Mordkovich, M. Baxendale, R. P. H. Chang, S. Yoshimura, *Synth. Met.* 86, 2049 **(1997)**

62. V. Z. Mordkovich, M. Baxendale, M. Yudasaka, S. Yoshimura, J.-Y. Dai, R. P. H. Chang, *Mol. Cryst. Liq. Cryst.* 310, 159 **(1998)**

63. V. Z. Mordkovich, *Mol. Cryst. Liq. Cryst.* 340, 775 **(2000)**

64. V. Z. Mordkovich, *Mol. Mat.* 13, 95 **(2000)**

65. M. Baxendale, V. Z. Mordkovich, S. Yoshimura, R. P. H. Chang, A. G. M. Jansen, *Phys. Rev. B* 57 (24), 15629 **(1998)**

66. M. Baxendale, G. A. J. Amaratunga, *Synth. Met.* 103, 2496 **(1999)**

67. D. Claves, J. Giraudet, M. C. Schouler, P. Gadelle, A. Hamwi, *Solid State Commun.* 130, 1 **(2004)**

68. J. Giraudet, M. Dubois, D. Claves, J. P. Pinheiro, M. C. Schouler, P. Gadelle, A. Hamwi, *Chem. Phys. Lett.* 381, 306 **(2003)**

69. Z. Chen, X. Du, M.-H. Du, C. D. Rancken, H.-P. Cheng, A. G. Rinzler, *Nanolett.* 3 (9), 1245 **(2003)**

70. Y. Yang, H. Zou, B. Wu, Q. Li, J. Zhang, Z. Liu, X. Guo, Z. Du, *J. Phys. Chem. B* 106 (29), 7160 **(2002)**

71. J. G. Wiltshire, A. N. Khlobystov, L. J. Li, S. G. Lyapin, G. A. D. Briggs, R. J. Nicholas, *Chem. Phys. Lett.* 386, 239 **(2004)**

72. K. H. An, C.-M. Yang, J. S. Park, S. Y. Jeong, Y. H. Lee, *J. Phys. Chem. B* 109 (20), 10004 **(2005)**

73. K. H. An, J. S. Park, C.-M. Yang, , S. Y. Jeong, S. C. Lim, C. Kang, J.-H. Son, M. S. Jeong, Y. H. Lee, *J. Am. Chem. Soc.* 127 (14), 5196 **(2005)**

74. C. M. Yang, J. S. Park, K. H. An, S. C. Lim, K. Seo, B. Kim, K. A. Park, S. Han, C. Y. Park, Y. H. Lee, *J. Phys. Chem. B* 109 (41), 19242 **(2005)**

75. G. Zhou, W. Duan, J. Nanosci. *Nanotechnol.* 5 (9), 1421 **(2005)**

76. D. Claves, F. Chamssedine, M. C. Schouler, A. Hamwi, to be published

77. Q. Zhu, D. E. Cox, J. E. Fischer, K. Kniaz, A. R. McGhie, O. Zhou, *Nature* 355, 712 **(1992)**

78. M. Kobayashi, Y. Akahama, H. Kawamura, H. Shinohara, H. Sato, Y. Saito, *Solid State Commun.* 81 (1), 93 **(1992)**

79. M. Kobayashi, Y. Akahama, H. Kawamura, H. Shinohara, H. Sato, Y. Saito, *Mat. Sc. Eng. B* 19, 100 **(1993)**

80. Y. Akahama, M. Kobayashi, H. Kawamura, H. Shinohara, H. Sato, Y. Saito, *Solid State Commun.* 82 (8), 605 **(1992**)

81. Y. S. Grushko, G. Wortmann, M. F. Kovalev, L. I. Molkanov, Y. V. Ganzha, Y. A. Ossipyan, O. V. Zharikov, *Solid State Commun.* 84 (5), 505 **(1992)**

82. M. Seto, Y. Maeda, T. Matsuyama, H. Yamaoka, H. Sakai, *Synth. Met.* 55-57, 3167 **(1993)**

83. P. V. Huong, *Solid State Commun.* 88 (1), 23 **(1993)**

84. S. Nakashima, M. Norimoto, H. Harima, Y. Hamanaka, L. S. Grigoryan, M. Tokumoto, *Chem. Phys. Lett.* 268, 359 **(1997)**

85. N.-G. Park, S.-W. Cho, S.-J. Kim, J.-H. Choy, *Chem. Mat.* 8 (2), 324 **(1996)**

86. H. Sekine, H. Maeda, M. Kosuge, Y. Tanaka, M. Tokumoto, *J. Appl. Phys.* 72 (11), 5448 **(1992)**

87. H. Sekine, H. Maeda, M. Kosuge, Y. Tanaka, M. Tokumoto, *Synth. Met.* 55-57, 3068 **(1993)**

88. M. Tokumoto, N. Kinoshita, Y. Tanaka, S. Ishibashi, H. Ihara, H. Sekine, H. Maeda, *Synth. Met.* 70, 1387 **(1995)**

89. Y. Maniwa, Y.-S. Tae, K. Kume, H. Sekine, *Solid State Commun.* 93 (2), 103 **(1995)**

90. A. Hamwi, G. Dondainas, J. Dupuis, *Mol. Cryst. Liq. Cryst.* 245, 301 **(1994)**

91. A. Hamwi, C. Latouche, B. Burteaux, J. Dupuis, *Fullerenes Science Technol.* 4 (6), 1213 **(1996)**

92. B. Burteaux, A. Hamwi, D. Avignant, J. Dupuis, *Mol. Cryst. Liq. Cryst.* 310, 137 **(1998)**

93. A. Hamwi, D. Claves, *J. Fluor. Chem.* 107, 241 **(2001)**

94. W. R. Datars, T. R. Chien, R. K. Nkum, P. K. Ummat, *Phys. Rev. B* 50 (7), 4937 **(1994)**

95. W. R. Datars, P. K. Ummat, *Solid State Commun.* 94 (8), 649 **(1995)**

96. R. Francis, W. R. Datars, *Solid State Commun.* 103 (4), 219 **(1997)**

97. A. M. Panich, P. K. Ummat, W. R. Datars, *Solid State Commun.* 121, 367 **(2002)**

98. A. M. Panich, H.-M. Vieth, P. K. Ummat, W. R. Datars, *Physica B* 327, 102 **(2003)**

99. R. Francis, P. K. Ummat, W. R. Datars, *J. Phys. Condens. Matter* 9, 7223 **(1997)**

100. A. M. Panich, I. Felner, A. I. Shames, S. Goren, P. K. Ummat, W. R. Datars, *Solid State Commun.* 129, 81 **(2004)**

101. J. C. L. Chow, P. K. Ummat, W. R. Datars, *J. Phys. Condens. Matter* 12, 8551 **(2000)**

102. W. R. Datars, P. K. Ummat, T. Olech, R. K. Nkum, *Solid State Commun.* 86 (9), 579 **(1993)**

103. W. R. Datars, J. D. Palidwar, P. K. Ummat, *J. Phys. Chem. Solids* 57 (6-8), 977 **(1996)**

104. M. Barati, P. K. Ummat, W. R. Datars, *Solid State Commun.* 106 (2), 91 **(1998)**

105. W. Maser, S. Roth, J. Anders, J. Reichenbach, M. Kaiser, H. Byrne, H. Schier, M. Filzmoser, E. Sohmen, J. Fink, P. Bernier, A. Zahab, H.-U. Siehl, M. Hanack, *Synth. Met.* 51, 103 **(1992)**

106. R. D. Bolskar, R. S. Mathur, C. A. Reed, *J. Am. Chem. Soc.* 118 (51), 13093 **(1996)**

107. C. A. Reed, K.-C. Kim, R. D. Bolskar, L. J. Mueller, *Science* 289, 101 **(2000)**

108. O. V. Boltalina, I. N. Ioffe, L. N. Sidorov, G. Seifert, K. Vietze, *J. Am. Chem. Soc.* 122 (40), 9745 **(2000)**

109. R. Saito, G. Dresselhaus, M. S. Dresselhaus, *Phys. Rev. B* 46 (15), 9906 **(1992)**

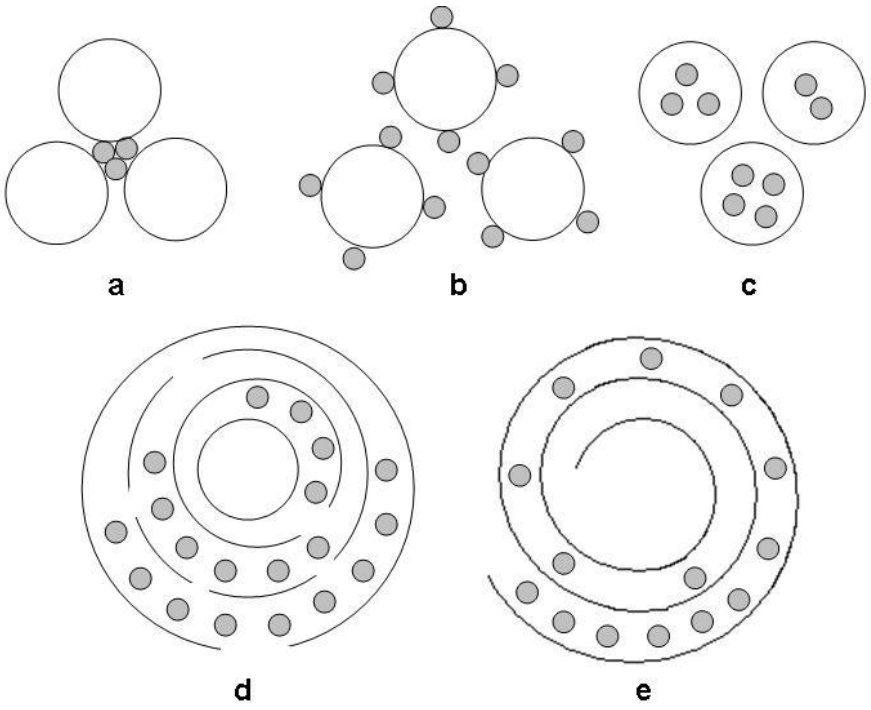

Fig. 1. Topological description of the intercalation into SWNTs ropes and MWNTs a) filling of the interstitial channels b) covering of the outer surface c) filling of the inner core d) anisotropic radial distribution of intercalates within a MWNT presenting extended wall disruptions e) diffusion into the spiroïdal interlayer space of a scroll MWNT.

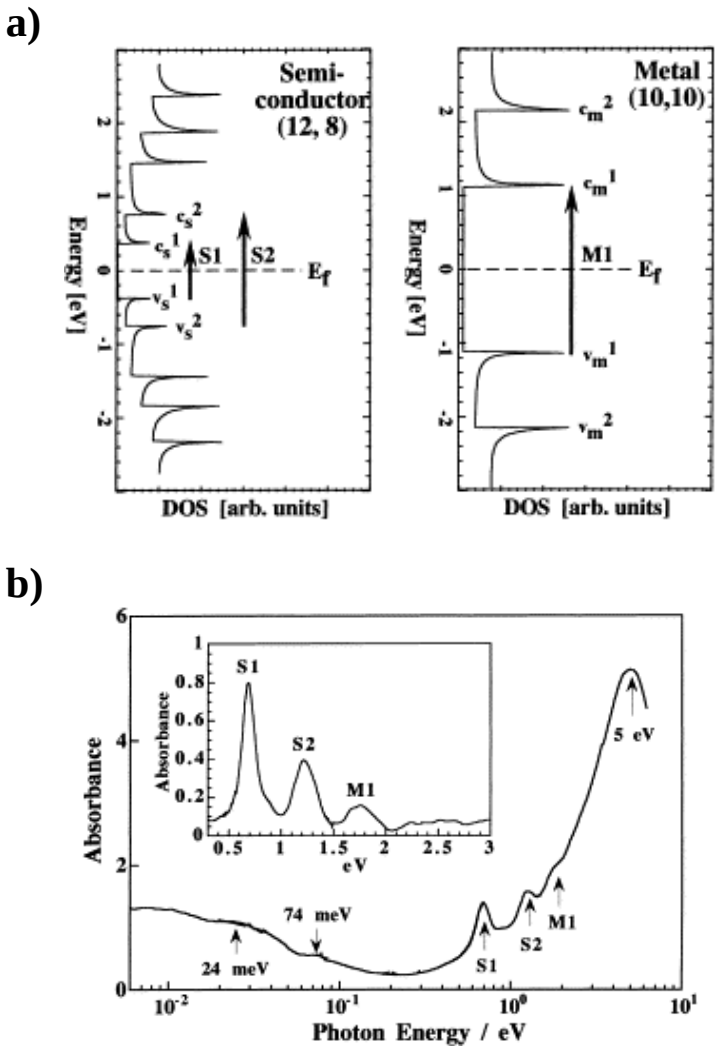

Fig. 2. Calculated DOS for a semiconducting (12,8) or metallic (10,10) SWNT and illustration of the first optically allowed transitions between the corresponding van Hove singularities. Reprinted with permission from Ref. 7, N. Minami et al., *Synth. Met.* 116, 405 (2001). Copyright © Elsevier.

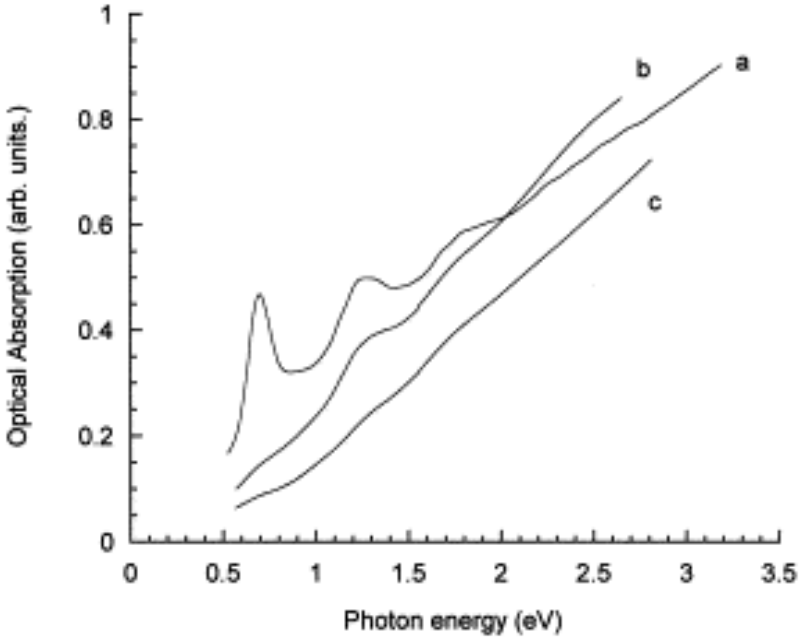

Fig. 3. Illustration of the effect exerted by a) iodine and c) bromine-doping on the optical absorption features of b) pristine SWNTs. Reprinted with permission from Ref. 12, P. Petit et al., *Chem. Phys. Lett.* 305, 370 (1999). Copyright © Elsevier.

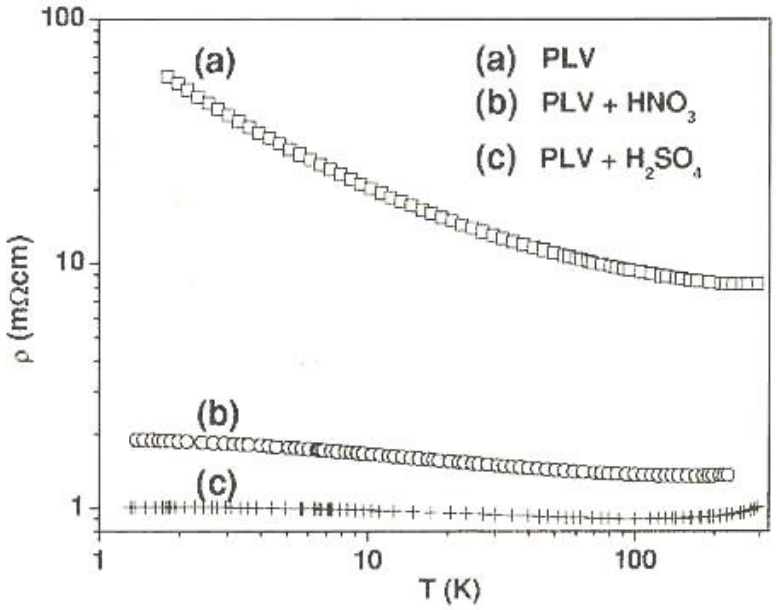

Fig. 4. Effect of doping with Brönsted acids on the resistivity of SWNTs samples grown by pulsed laser vaporization (PLV), and its temperature dependence. Reprinted with permission from Ref. 29, W. Zhou et al., *Phys. Rev. B* 71, 205423 (2005). Copyright © American Physical Society.

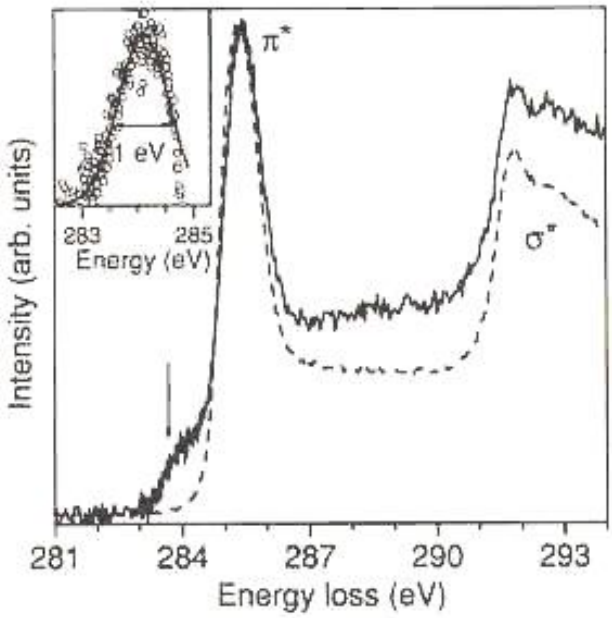

Fig. 5. Visualization, through C_{1s} core-level excitations, of the emergence of novel empty states (arrow), upon doping of a SWNTs film with gaseous ferric chloride (dashed and solid lines refer to pristine and $FeCl_3$-doped SWNTs, respectively). Reprinted with permission from Ref. 43, X. Liu et al., *Phys. Rev. B* 70, 205405 (2004). Copyright © American Physical Society.

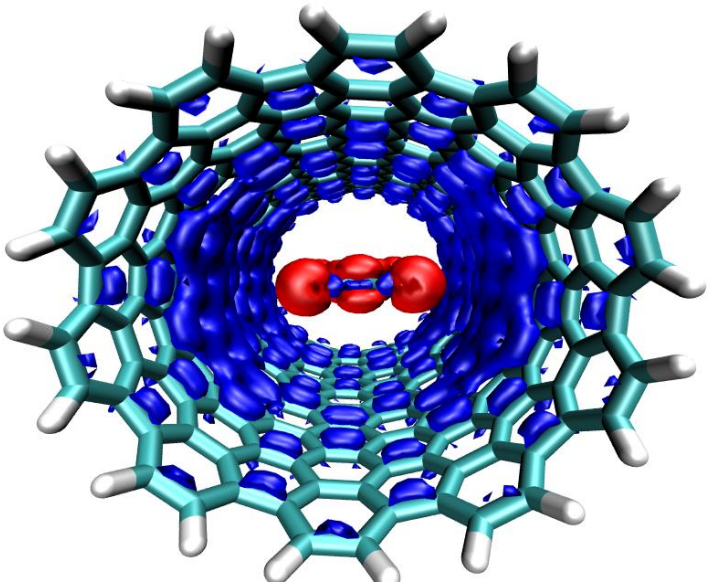

Fig. 6. Charge-density isosurfaces calculated upon encapsulation of a $TCNQF_4$ molecule into a SWNT segment, showing charge transfer to the dopant. The red/blue zones correspond to excess/deficit of electron density. Reprinted with permission from Ref. 52, V. Meunier et al., *J. Chem. Phys.* 123, 024705-1 (2005).

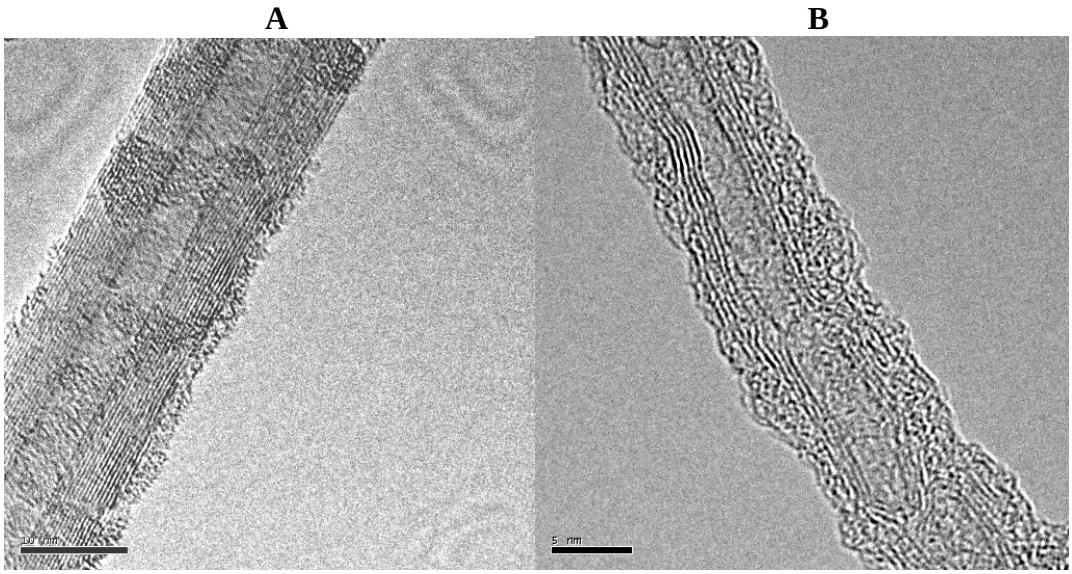

Fig. 7. TEM micrographs of MWNTs samples issued from different synthesis techniques: A) Arc-discharge process B) low temperature CVD process showing an abundance of defects enhancing chemical reactivity.

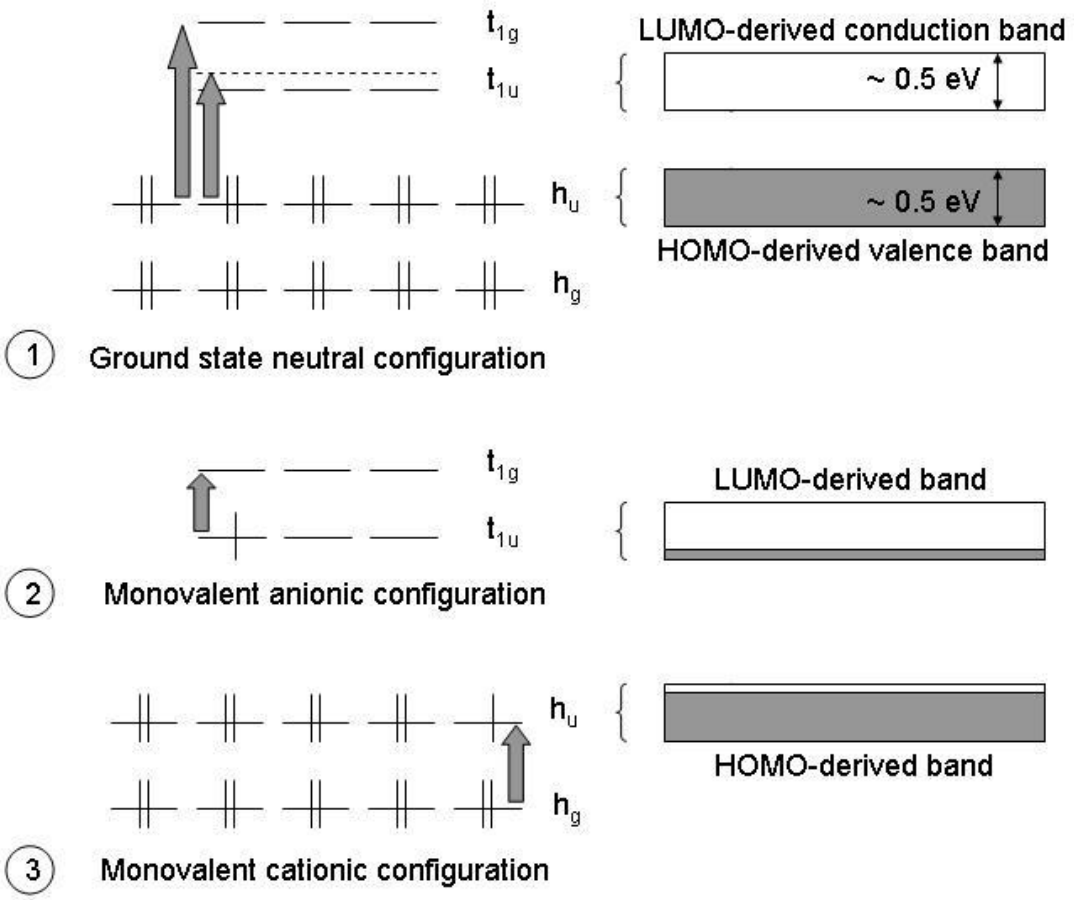

Fig. 8. Schematic illustration of the modifications induced upon charging i) in the closed shell ground electronic state of the isolated [60]fullerene cluster ii) in the related optical transitions (arrows) occurring in the Vis-NIR region (N.B: $h_u \rightarrow t_{1u}$ is a "vibrationally-assisted" parity-forbidden transition, of weak intensity) and iii) in the corresponding rigid band structure description in the condensed state.